Scientific Reports

https://doi.org/10.1038/s41598-026-43979-7

Article in Press

Study on the influence of composite charge structure and initiation mode on the kinetic energy conversion efficiency of shell

Received: 10 April 2025

Accepted: 9 March 2026

Published online: 11 March 2026

Cite this article as: Zhao L., Yin J. & Li X. Study on the influence of composite charge structure and initiation mode on the kinetic energy conversion efficiency of shell. *Sci Rep* (2026). https://doi.org/10.1038/s41598-026-43979-7

Lichen Zhao, Jianping Yin & Xudong Li

Article

Study on the Influence of Composite Charge Structure and Initiation Mode on the Kinetic Energy Conversion Efficiency of Shell

Lichen Zhao [1], Jianping Yin [1,*] and Xudong Li [1]

1 College of Mechanical and Electrical Engineering, North University of China, Taiyuan 030051, China; zlc199703@163.com(L.Z); lxdscibizhong@126.com(X.L)
*Correspondence: yjp123@nuc.edu.cn

Abstract: This paper mainly investigates the influence of initiation mode and structural parameters of composite charge on detonation waveform and kinetic energy conversion efficiency of driving shell. The simulation was carried out by using AUTODYN software. The results provided the detonation waveform and the final kinetic energy of the shell under different charge structure parameters and initiation mode, and the kinetic energy conversion efficiency from the initial energy of the composite charge to the kinetic energy of the shell was calculated. The orthogonal optimization method is used to study and analyze the kinetic energy and kinetic energy conversion efficiency of the shell with three factors and each level, and the best parameter combination scheme is obtained. The three factors are the detonation velocity matching relationship between the inner and outer explosives of the composite charge, the initiation mode and the loading ratio of the inner and outer explosives. From the perspective of detonation waveform, the results show that when the inner layer is high detonation velocity explosive and the outer layer is low detonation velocity explosive, the detonation waveform is convex wave. On the contrary, under the explosive matching relationship of low detonation velocity in the inner layer and high detonation velocity in the outer layer, the detonation waveform is concave wave. From the perspective of the kinetic energy conversion efficiency of the shell, the results show that the kinetic energy conversion efficiency of the shell is the largest under the charge structure with the inner layer of low detonation velocity explosive and the outer layer of high detonation velocity explosive, loading ratio of the inner and outer explosives is 0.25 and the initiation mode is the initiation of the center point at the bottom of both ends. The research results can provide support for the design of composite charge structure.

Keywords: Detonation waveform; Detonation mode; Composite charge structure; Kinetic energy conversion efficiency

1. Introduction

The propagation of detonation waveform is a key phenomenon in the process of explosion. The charge structure and initiation mode are important factors affecting the propagation of detonation waveform, which directly determine the propagation law, pressure and energy release of detonation waveform. The energy output characteristics of a single charge structure are basically fixed, and the means of regulating the detonation waveform are limited. However, for a composite charge structure, the detonation waveform can be changed by regulating the charge structure and initiation mode of the inner and outer layers of explosives. Therefore, in order to optimize the detonation waveform and improve the kinetic energy conversion efficiency of the shell, it is necessary to carry out research on the charge structure and initiation mode of the inner and outer layer explosives for regulating the composite charge.

Optimizing the initiation mode design to change the detonation waveform and then studying the output characteristics of explosion energy is one of the main research directions in this field now. At present, a large number of scholars are focusing on studying the regulation of detonation waveforms by changing the initiation mode, and then investigate the characteristics of detonation energy output. Gu et al. [1] studied the distribution law of explosion shock wave field by changing the single detonation and combined detonation when the warhead is a single charge TNT. Li et al [2] studied the propagation law of shock wave and the influence of overpressure field distribution under the single charge trapezoidal warhead by means of multi-point detonation on the central axis. In the case of a single charge of the warhead, Wang et al. [3] analyzed the influence of different detonation mode on the distribution of the

initial velocity of the fragment along the axial direction of the warhead, and then studied the influence of the detonation method on the lethality of the warhead. Miu [4] studied the influence of bilinear symmetric detonation mode on the propagation characteristics of axial detonation waveform and the distribution of detonation pressure of strip charge with single charge. Deng et al. [5] studied the fragment velocity distribution and energy output characteristics of the warhead with elliptical cross section under different detonation modes. Guo et al. [6] studied the variation laws of internal and external detonation pressures of explosives under symmetrical bilinear initiation and unilateral linear initiation methods for a single charge. Xiao et al. [7] investigated the changes in detonation waveforms and detonation pressures under the charge structure of a single explosive 8701 by studying the initiation mode at one end and both ends. Li et al. [8] studied the axial propagation characteristics of a single charge detonation waveform by means of symmetrical bilinear initiation. Li et al. [9] studied the fragmentation and shock wave characteristics of composite charges by changing two initiation modes: one that only detonates the inner layer of explosives and the other that simultaneously detonates the inner and outer layers of explosives. Zhang et al. [10] studied the influence of non-circular cross-section charge structures on the evolution of detonation waveforms, fragment mass and initial velocity of fragments under different initiation modes by changing the single-point initiation at the end, two-point initiation and three-point initiation. Deng et al. [11] investigated the propagation, superposition and fragmentation velocity of detonation waveforms under single-layer charge by studying four different eccentric initiation methods. It can be seen that the current method of optimizing the initiation mode and thereby regulating the waveform has broad prospects and significance for improving the velocity distribution, overpressure distribution, debris mass and motion distribution of the shell.

In addition to the initiation mode, the charge structure also has a significant impact on the propagation characteristics of the detonation waveform. The propagation process of the detonation waveform within the charge structure is restricted by multiple factors such as the internal structure of the composite charge and the properties of the explosive material. Different charge structures will directly affect the pressure distribution, waveform characteristics and energy release of the detonation waveform. Therefore, optimizing the charge structure design, enhancing the propagation efficiency of detonation waveforms, and improving the energy output characteristics are important research directions in this field. In terms of the regulation of charging structure parameters, Zhang [12] studied the detonation energy output and shock wave sensitivity of the composite charge by changing the radius ratio and height ratio of the inner and outer layers of the high-sensitivity explosive based on HMX and the insensitive explosive based on TATB. Yin [13] studied the fragment driving ability and shock wave overpressure characteristics in the fully prefabricated composite charge fragment warhead through simulation and experiment. Niu [14] studied the variation of underwater explosion shock wave by making GH-1 and GUHL-1 explosives into a composite charge structure with inner and outer layers and upper and lower superposition. Shen et al. [15] obtained the detonation release law of 3,4-dinitrofurazanfuroxan (DNTF) based high detonation velocity explosive and high detonation heat explosive by narrow scanning experiment and circular experiment. Hamada [16] studied the overpressure detonation process of composite charge with outer layer of high detonation velocity explosive and inner layer of low detonation velocity explosive. The results show that the overpressure detonation pressure of composite charge is 2.5 times that of CJ detonation pressure. Shi et al. [17] conducted two-point detonation of composite cylindrical explosives containing RDX, Al powder, etc., so as to study the enhancement effect of near-field shock wave power of explosives. Li et al [18] studied the energy output characteristics of coaxial composite charge with shell under different detonation modes with polyurethane material as the explosion-proof material, and the inner layer is 8701 explosive and the outer layer is RDX-based aluminized explosive. Shen et al. [19] obtained the detonation waveform propagation characteristics of coaxial double charge structures prepared by two types of aluminum-containing explosives with a detonation velocity difference of 1.81mm/ microsecond between the inner and outer layers by using high-speed scanning method and electrical measurement method, respectively. Wang [20] studied the stable propagation of detonation waveforms and the expansion process of the cylinder in a single-layer PBX cylinder through a combination of simulation and experiments. Ling et al. [21] studied the dispersion characteristics of detonation waveform trace fragments by altering the structural parameters of fan-shaped single and composite charges. Lu et al. [22] studied the fragmentation velocity by altering the mass ratio of the charge inside a cylinder. Zhao et al. [23] studied the propagation and action process of detonation waveforms by adding different partitions in the composite charge structure.

At present, most scholars focus on simply changing the initiation mode of the charge or attempting to regulate the detonation waveform by adjusting the structure of the composite charge. However, there are relatively few studies that combine the different composite charge structure with the initiation mode to investigate the variation law of detonation waveforms. Especially, the research on artificially regulating the detonation waveform by combining the composite charge structure with the initiation mode to improve the kinetic energy conversion efficiency of the shell is relatively lacking. In this regard, in order to achieve the optimization of detonation waveforms and enhance the kinetic energy conversion efficiency of the shell, this paper discusses the influence of the optimized design of the composite charge structure and the initiation mode on the propagation of detonation waveforms and the kinetic energy of

the shell. Through numerical simulation of a specific composite charge structure, the effects of different initiation modes and the loading structures of inner and outer layers of explosives on the propagation of detonation waveforms, the kinetic energy of the shell and the kinetic energy conversion efficiency of the shell were evaluated. Taking the kinetic energy conversion efficiency of the shell as the index, different composite charge structures and initiation modes were evaluated, and the optimal combination of composite charge structures and initiation methods with high kinetic energy conversion efficiency of the shell was obtained, providing a research basis for optimizing the detonation waveform and exploring the energy conversion rate of explosives.

2. Composite Charge Structure Design

2.1. Composite Charge Structure

The composite charge structure used in this paper is shown in Figure 1, which mainly includes: inner explosive, outer explosive and shell. The composite charge is a coaxial multi-layer cylindrical structure with a height of 30 cm and a diameter of 11 cm. The thickness of the outer shell is 0.5 cm. The height of the inner and outer explosives is consistent with that of the shell. T1 and T2 represent the diameter of the inner explosive and the diameter of the outer explosive. The length of the T2 is 10 cm, and the length of the T1 is depends on the loading ratio of inner and outer explosives.

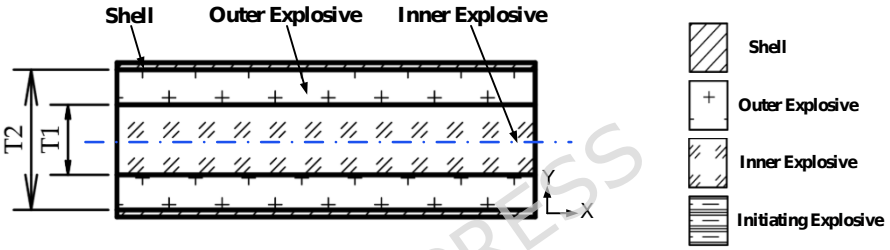

Figure 1. Structure Diagram of Composite Charge

2.2. Detonation Mode Design

In this paper, four kinds of initiation modes are used. As shown in Figure 2, there are four kinds of initiation modes, which are initiation of the center point at the bottom of one end, initiation of the surface at the bottom of one end, initiation of the center point at the bottom of both end and initiation of the internal center point. Because the explosive in the inner and outer layers of the composite charge is set as the explosive of the Lee Tarver equation of state, it cannot be directly initiated and can only be initiated by impact, so the initiation explosive HMX with the equation of state of JWL is set in the composite charge. The detonation waveform generated by the explosion of the explosive HMX initiation the inner and outer layers of explosives. The position of the initiation explosive changes according to the change of the initiation mode. Regarding the size of the initiation explosive, for both the initiation of the center point at the bottom of one end and the initiation of the center point at the bottom of both end, the size of the initiation explosive is 2cm along the X-axis and 3cm along the Y-axis. The initiation explosive size of the initiation of the internal center point is 4cm along the X-axis and 3cm along the Y-axis. The size of the initiation explosive for the initiation of the surface at the bottom of one end is 1.2cm along the X-axis and 10cm along the Y-axis. The position of the initiation explosive can be seen from Figure 2.

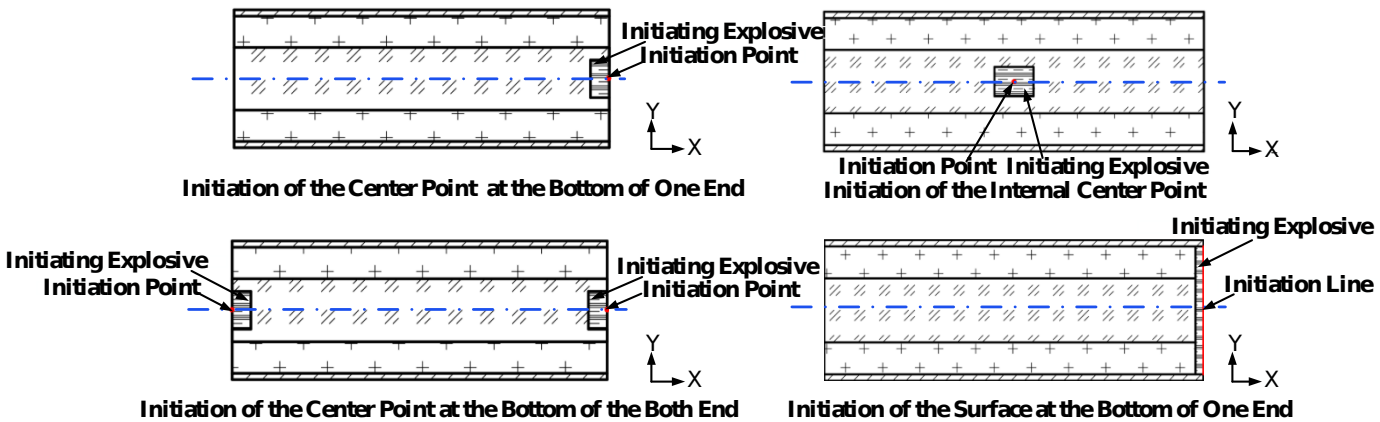

Figure 2. Four Initiation Modes

3. Finite Element Model Building

3.1. Establishment of Finite Element Model

AUTODYN (ANSYS 2022) software is used to numerically simulate the process of explosive explosion and detonation waveform propagation. The calculation adopts the coupling of EULER and Lagrange. The model scale is 1:1, and the unit system for modeling is cm-g-μs. There are three parts in the calculation domain, which are explosive, shell, and air. First, the air domain part is established using the Euler algorithm (a commonly used algorithm for flu-id substances). Next, the inner and outer layers of explosive and initiating explosive are directly added on the air domain. Then, the shell part is newly established using the Lagrange algorithm (a commonly used algorithm for solid substances), and the model is a 2D axisymmetric model. The Flow Out command is used to simulate the model with three free boundaries on the air domain. The overall grid size is set to 0.1 cm × 0.1 cm. Thirty-one Gauge observation points are set on the shell, and the interval between each Gauge observation point is 1cm. The diagram of the calculation model is shown in Figure 3.

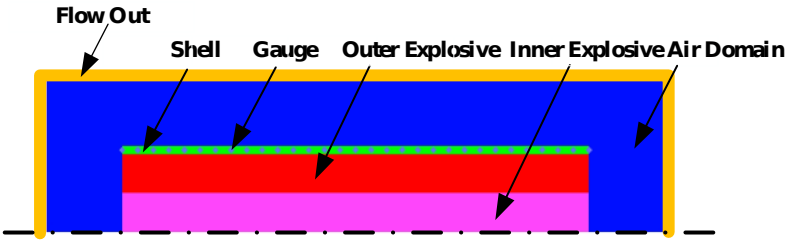

Figure 3. The Calculation Model Diagram

3.2 Material Model Selection

There are two kinds of explosives used in the inner and outer layers, CL20JJ1 explosive (hereinafter referred to as CL-20 explosive) and TNTCASTJJ1 explosive (hereinafter referred to as TNT explosive). CL-20 explosive has high detonation pressure, good safety and stability. TNT explosive also has high stability and strong safety. Both explosives can release a large amount of energy in a short time, produce significant destructive power, and have a large detonation velocity difference, about 2280m/s, so it can more clearly reveal the influence of high and low detonation velocity explosives on detonation waveforms. The HMX explosive was selected as the initiation explosive, and the COPPER material was used as the shell. In the study, AUTODYN simulation software was used to simulate the internal structure of the composite charge. In the simulation, all the materials are selected from the finite element software library, and the air adopts the ideal gas state equation. JWL and Lee Tarver state equations were used for explosives. The specific parameters of the explosive state equation are shown in Table 1 and Table 2. Table 3 is the selected shell material density, state equation, strength model and failure model.

The JWL equation of state is described as follows [24] :

$$p = A\left(1 - \frac{\omega}{R_1\nu}\right)e^{-R_1\nu} + B\left(1 - \frac{\omega}{R_2\nu}\right)e^{-R_2\nu} + \frac{\omega E}{\nu} \qquad (1)$$

In the formula, p is the product pressure, Mbar; ν is the relative specific volume of the product, m^3/kg; E is the specific internal energy of the product, Mbar; A, B, R_1, R_2 and ω are undetermined coefficients, which are obtained by cylinder experiment.

Table 1. Parameter of JWL Equation of State for HMX Explosive

Explosive	Detonation Velocity(m/s)	ρ (g/cm^3)	A (Mbar)	B (Mbar)	R_1	R_2	ω
HMX	9110	1.891	778.28	7.0714	4.2	1	0.3

The shock response process of explosive is simulated by Lee-Tarver trinomial ignition growth model., including the state equation of three stages. The first stage of the equation is the ignition stage. In the early stage of the impact initiation, the hot spot is generated and the ignition is completed due to the action of the incident shock wave. The second stage is the growth stage, which is the low-speed growth

stage of the hot spot outward diffusion; the third stage is the fast reaction stage, which spreads rapidly on the basis of the hot spots formed in the early stage, so that the unreacted samples can quickly complete the reaction and eventually grow into detonation. The trinomial ignition growth reaction rate equation has good compatibility with the JWL equation of state of reaction products and unreacted products, and is often used together to form a complete Lee-Tarver ignition growth model [25]. The reaction rate equation of state of CL-20 and TNT in this paper uses the above-described form. The specific equation is as follows [26]:

$$\frac{dF}{dt} = I(1 - F)^b(\mu - a)^x + G_1(1 - F)^cF^dp^y + G_2(1 - F)^eF^gp^z \qquad (2)$$

In the formula, F is the reaction ratio (the ratio of the mass of gas explosive to the total mass of explosive) ; $\mu = \frac{\rho}{\rho_0} - 1$，$\mu$ is used to characterize the compressibility of the material，ρ is the current density，g/cm^3，p is pressure, Mbar; I，b，a，x，G_1，c，d，y，G_2，e，g，z are constants, which can be obtained by parameter fitting through pull analysis.

Table 2. Explosive Parameters of Lee Tarver Equation of State

Explosive	Detonation Velocity(m/s)	ρ (g/cm^3)	I	b	a	x	G_1	c	d	y	G_2	e	g	z
CL-20	9210	1.942	7.43e11	0.667	0	20	1500	0.667	0.333	2	400	0.333	1	2
TNT	6930	1.63	50	0.222	0	4	0	0	0	0	40	0.222	0.666	1.2

Shock state equation is described as follows [27] :

$$\rho = \begin{cases} \rho_H + \Gamma_\rho(e - e_H), \mu \geq 0 \\ \rho_0 c_0 \mu, \mu < 0 \end{cases} \qquad (3)$$

In the formula,

$$\rho_H = \frac{\rho_0 c_0^2 \mu(1+\mu)}{[1-(s-1)\mu]^2}, e_H = \frac{1P_H}{2\rho_0}\left(\frac{\mu}{1+\mu}\right) \qquad (4)$$

Here, Γ is the Gruneisen coefficient, ρ_0 is the initial density, g/cm^3, $\mu = \rho/\rho_0 - 1$.

The Johnson-Cook constitutive model can better reflect the strain rate effect and temperature softening effect of the material, and the expression is as follows [28] :

$$\sigma = (A + B\varepsilon^n)[1 + C\ln\left(\frac{\dot{\varepsilon}}{\dot{\varepsilon}_0}\right)][1 - (T^*)^m] \qquad (5)$$

In the formula, σ is the true stress, Mbar, A is the yield stress under the reference condition, Mbar, B and n are the strain hardening coefficient and strain hardening index, respectively. ε is the true strain, C is the strain rate strengthening coefficient, $\dot{\varepsilon}$ is the actual strain rate, $\dot{\varepsilon}_0$ is the reference strain rate, m is the temperature rise softening coefficient, $T^* = (T - T_r)/(T_m - T_r)$, T is the experimental temperature, K, T_r is the reference temperature, K, and T_m is the material melting temperature, K.

Table 3. Material Parameters and Models Used in Calculation

Material	ρ (g/cm^3)	Equation of State	Strength Model	Failure Model

COPPER	8.9	Shock	Johnson Cook	Plastic Strain

In order to analyze the influence of grid size on the numerical simulation, in this study, seven grid sizes of 0.1 cm, 0.2cm, 0.3cm, 0.4cm, 0.5cm, 0.6cm and 0.7cm were selected to establish numerical simulation models under the same charge structure and model. The maximum pressure values at the same gauge point position in seven numerical simulation results were compared, and the comparison results are shown in Figure 4.

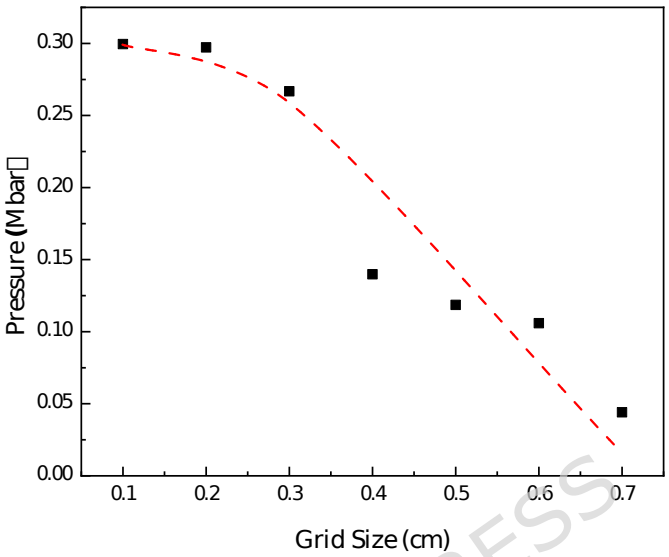

Figure 4. Grid Size Sensitivity Analysis

It can be seen from Figure 4, as the grid size decreases, the pressure value gradually tends to stabilize. When the grid size gradually decreases from 0.7 to 0.1, the corresponding pressure value keeps increasing. When the side length of the grid becomes 0.1cm, the pressure value tends to converge. Based on this, the numerical simulation in this paper ultimately adopts a grid with a side length of 0.1cm, which is reliable and reasonable.

To verify the accuracy of the numerical model, this study conducted a comparative verification of the incident shock wave overpressure time-history curve and detonation waveforms based on references [29] and [30]. As shown in Figure 5, it is a comparison of detonation waveform simulations conducted under the same charge structure and model. The first line is the detonation waveform numerical simulation diagram of this article, and the second line is the detonation waveform diagram in reference [29]. By comparing this two, it can be seen that at the same moment, the detonation waveforms have similar contours.

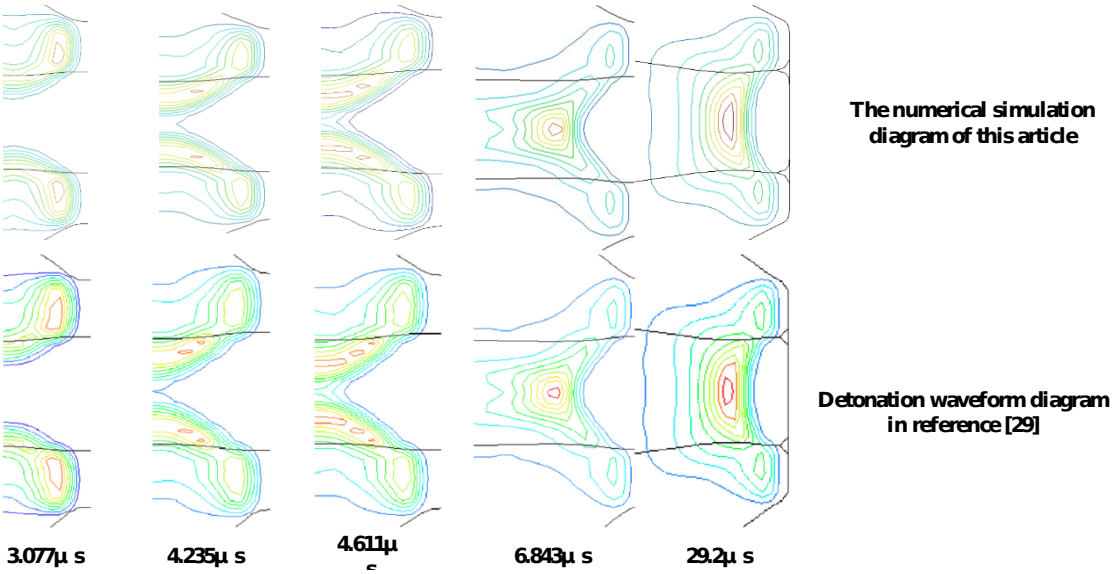

Figure 5. The comparison chart of detonation waveforms in the numerical simulation of this article with those in reference [29].

Then compare the incident shock wave overpressure time-history curves. Field experiments were conducted with reference [30], and the overpressure of the incident shock wave was tested. As shown in Figure 6, it is a numerical simulation and experimental comparison chart of the incident shock wave overpressure time-history curve under the same charge structure and model.

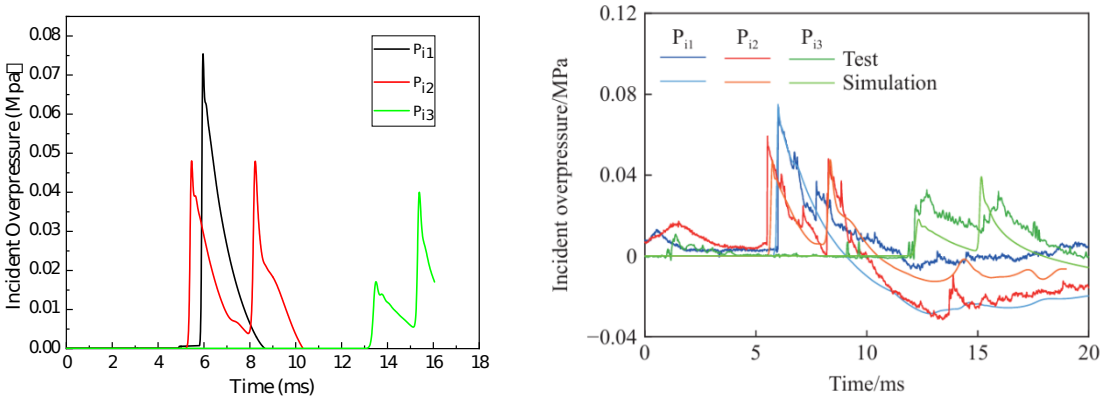

a) Numerical Simulation Diagram b) Experiment Diagram [30]

Figure 6. Numerical Simulation and Experimental Comparison Chart of the Incident Shock Wave Overpressure Time-History Curve

It can be seen from Figure 6 that the changing trends of the shock wave overpressure time-history curves presented by the numerical simulation and the test results are very similar.

According to the detonation waveforms have similar contours between the numerical simulation diagram of the detonation waveform in Figure 5 and the comparison diagram of the detonation waveform in reference [29], and the variation trend of the shock wave overpressure time-history curve presented by the numerical simulation and the test results in Figure 6 is very similar, the accuracy of the numerical simulation method can be determined.

In this paper, the air domain all choose is 50cm * 50cm square. Figure 7 shows the detonation waveform and the position distribution of the material in the air domain. It can be seen from Figure 7 that the detonation waveform and material distribution do not exceed the range of the air domain, which can support the complete driving acceleration of the shell.

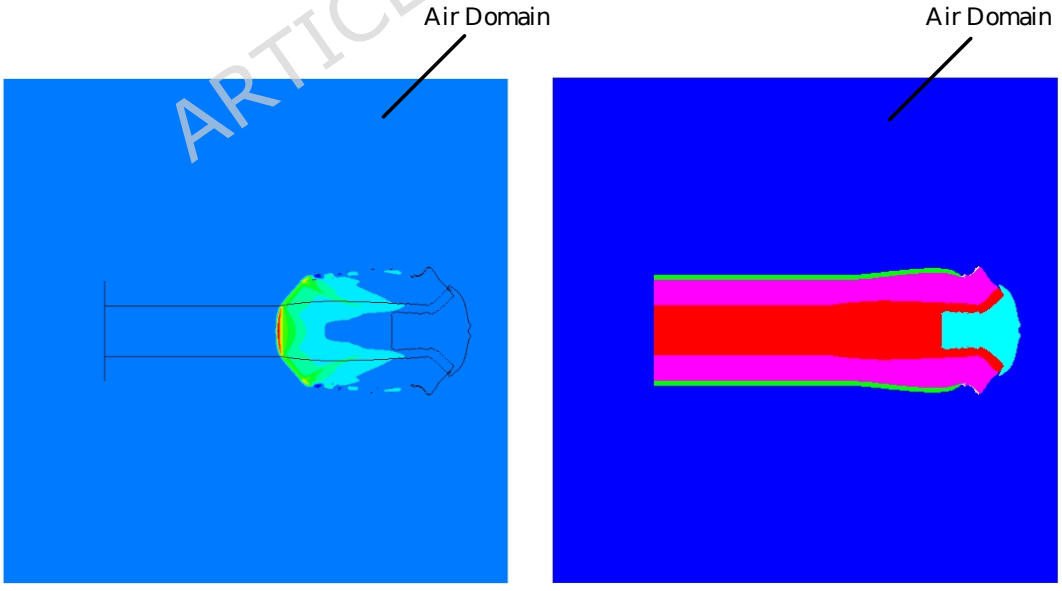

a) Detonation waveform diagram（ Scheme 1) b) Material Distribution diagram（ Scheme 1)

Figure 7. Detonation Waveform and Position Distribution of the Material in the Air Domain Diagram

4. Simulation Condition Design

In this part, the simulation calculation is mainly carried out by controlling the matching relationship between the detonation velocity of the inner and outer explosives, the loading ratio of the inner and outer explosives and the initiation mode. A total of two explosives were used, of which the high detonation

velocity explosive was CL-20 and the low detonation velocity explosive was TNT. In the design conditions, when the inner layer is a low detonation velocity explosive TNT and the outer layer is a high detonation velocity explosive CL-20, the following is referred to as the "Inner Low and Outer High". Similarly, the "Inner High and Outer Low" can be obtained.

In this paper, the matching relationship of detonation velocity, the loading ratio of inner and outer explosives and the initiation mode are selected as three factors, which are represented by A, B and C respectively. Factor A set two variables, factor B and factor C set four variables respectively. Each variable is represented by 1, 2, 3, 4. For example, B1, B2, B3 and B4 represent the four levels of the loading ratio of the inner and outer explosives, respectively. Similarly, the two levels of the detonation velocity matching relationship and the four levels of the detonation mode are also the same. The three factors affecting the detonation waveform and the corresponding levels of each factor are determined as shown in Table 4.

Table 4. Factor Level Design Table

	Detonation Velocity Maching Relationship A	**Loading Ratio of Inner and Outer Explosives B (T1:T2)**		**Initiation Mode C**
Level 1	A1 Inner High and Outer Low	B1	0.5	C1 Initiation of the Center Point at the Bottom of One End
Level 2	A2 Inner Low and Outer High	B2	0.334	C2 Initiation of the Center Point at the Bottom of Both End
		B3	0.25	C3.Initiation of the Internal Center Point
		B4	0.2	C4 Initiation of the Surface at the Bottom of One End

According to the number of factors and levels, a total of 32 schemes is designed as shown in Table 5.

Table 5 Scheme Design Table

Scheme	**Working Condition**	**Scheme**	**Working Condition**	**Scheme**	**Working Condition**	**Scheme**	Working **Condition**
1	A1,B1,C1	9	A1,B3,C1	17	A2,B1,C1	25	A2,B3,C1
2	A1,B1,C2	10	A1,B3,C2	18	A2,B1,C2	26	A2,B3,C2
3	A1,B1,C3	11	A1,B3,C3	19	A2,B1,C3	27	A2,B3,C3
4	A1,B1,C4	12	A1,B3,C4	20	A2,B1,C4	28	A2,B3,C4
5	A1,B2,C1	13	A1,B4,C1	21	A2,B2,C1	29	A2,B4,C1
6	A1,B2,C2	14	A1,B4,C2	22	A2,B2,C2	30	A2,B4,C2
7	A1,B2,C3	15	A1,B4,C3	23	A2,B2,C3	31	A2,B4,C3
8	A1,B2,C4	16	A1,B4,C4	24	A2,B2,C4	32	A2,B4,C4

5. Numerical Simulation Results Analysis

This part is mainly analyzed from two aspects. The first is about the composite charge under the same detonation velocity matching relationship, changing the initiation mode and the loading ratio of the inner and outer explosives, and observing the influence on the detonation waveform. Secondly, the influence of the loading ratio and initiation mode of the inner and outer explosives on the kinetic energy conversion efficiency of the shell is analyzed under the same matching relationship of the detonation velocity of the composite charge with the same inner high and outer low.

5.1. Propagation Process of Detonation Waveform of Composite Charge

5.1.1 The Propagation Process of Detonation Waveform at "Inner High and Outer Low''

When the inner layer of the composite charge is a high detonation velocity explosive CL-20 and the outer layer is a low detonation velocity explosive TNT, the initiation mode and the loading ratio of the inner and outer explosives are changed. The specific detonation waveform diagram is shown in Figure 8.

The transverse detonation waveform diagram has the same initiation mode, and the longitudinal detonation waveform diagram has the same charge ratio of inner and outer explosives.

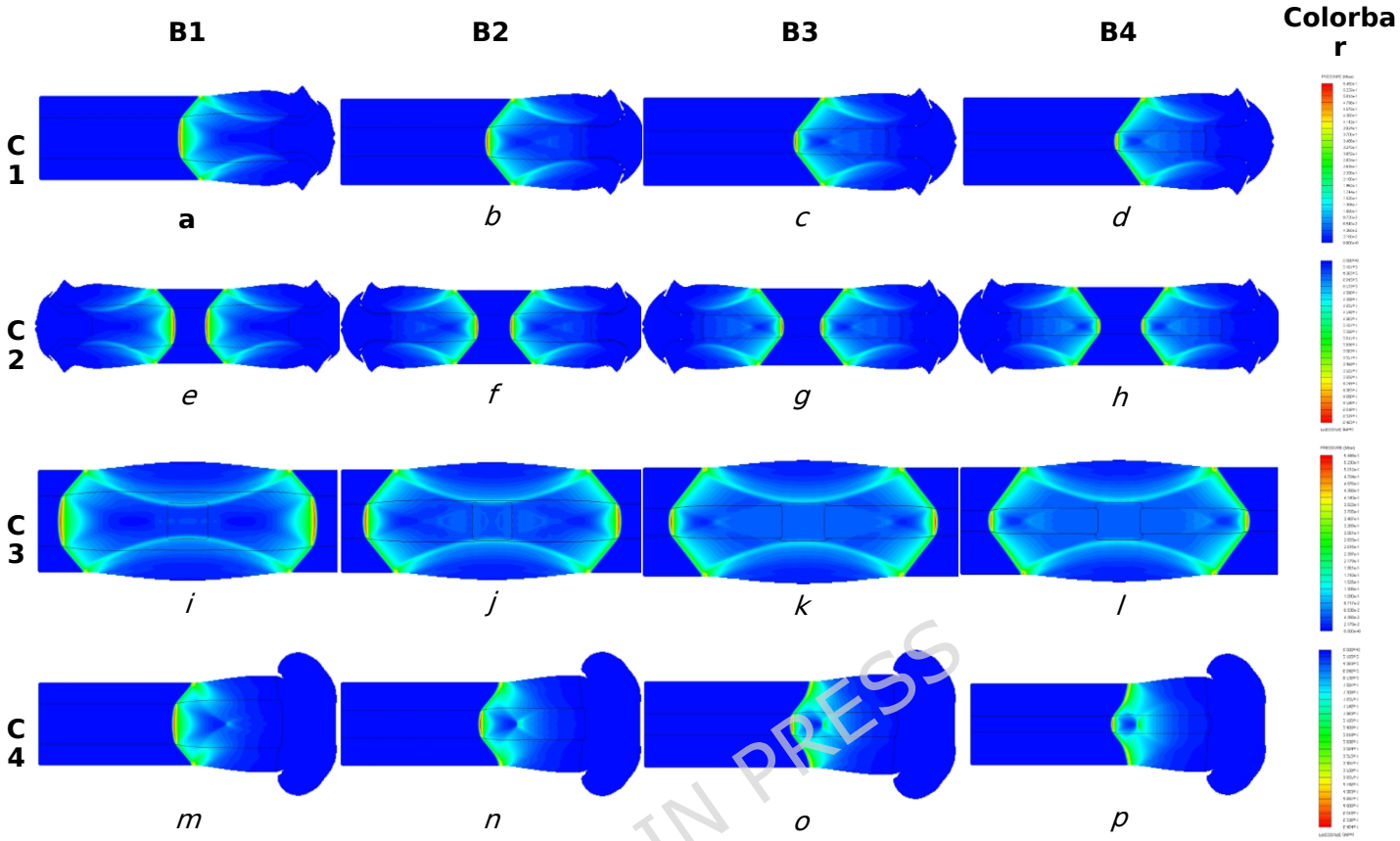

Figure 8. Detonation Waveform Propagation Diagram of “Inner High and Outer Low” Scheme

It can be seen from Figure 8 that different detonation modes will produce different detonation waveforms. Under the detonation velocity matching mode of "Inner High and Outer Low", no matter what kind of initiation mode and explosive loading ratio, the overall detonation waveform is convex wave. A convex waveform is formed by initiation of the center point at the bottom of one end. In the way of initiation of the center point at the bottom of both ends, the detonation waveform is generated from the bottom of both ends at the same time, forming a convex wave with two opposite directions. In the way of initiation at the internal center point, the detonation waveform is emitted from the internal center to both ends, and two convex waves in opposite directions are formed. A convex wave is formed by initiation at the one end bottom surface. And with the decrease of the loading ratio of the inner and outer layers of explosives, the overall convex wave is not smooth.

5.1.2The Propagation Process of Detonation Waveform at “Inner Low and Outer High”

When the inner layer of the composite charge is a low detonation velocity explosive TNT and the outer layer is a high detonation velocity explosive CL-20, the initiation mode and the loading ratio of the inner and outer explosives are changed. The specific detonation waveform diagram is shown in Figure 9.

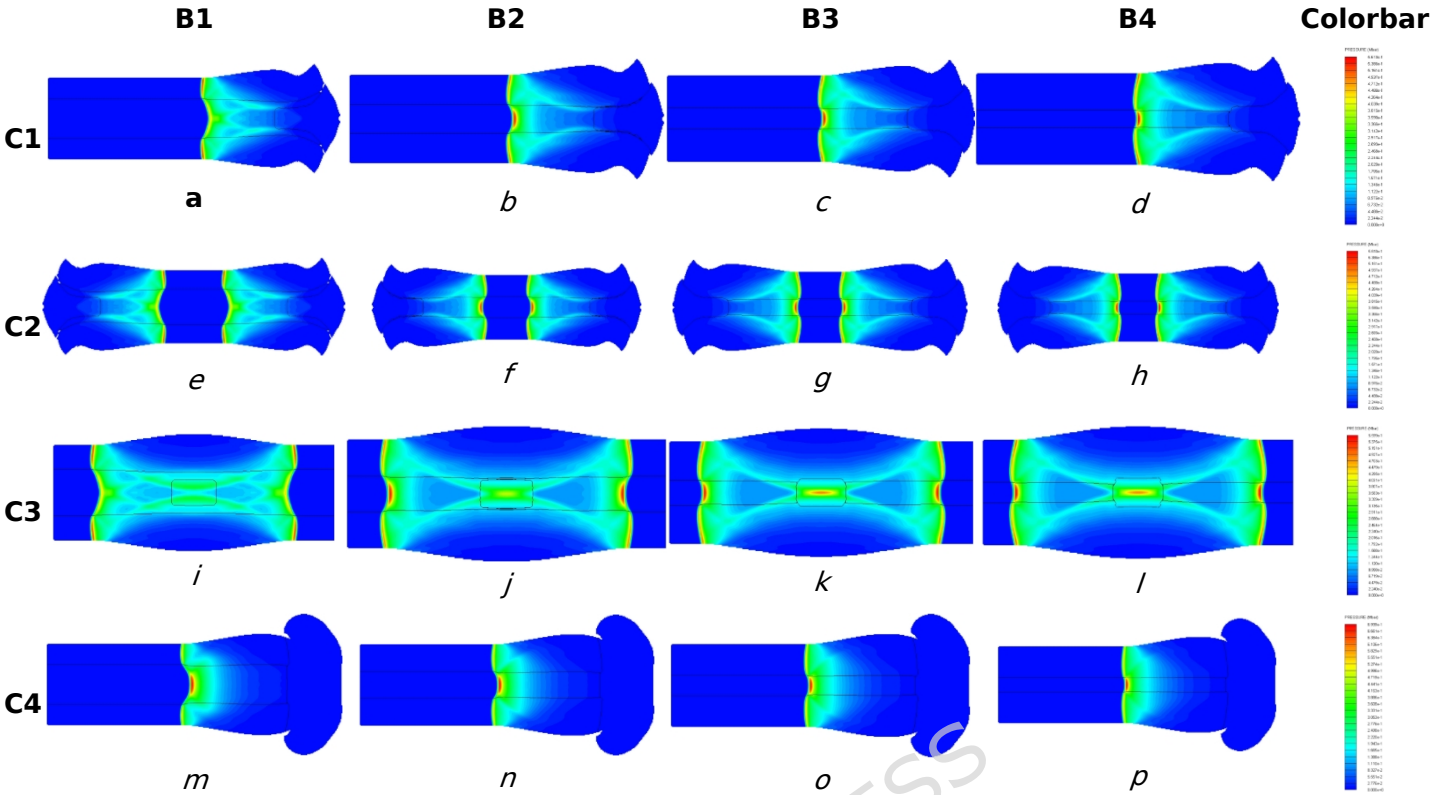

Figure 9. Detonation Waveform Propagation Diagram of "Inner Low and Outer High" Scheme

It can be seen from Figure 9 that the overall detonation waveform is a concave wave under the detonation velocity matching mode of "Inner Low and Outer High", no matter what kind of detonation mode and the loading ratio of inner and outer explosives. With the decrease of the loading ratio of the inner and outer explosives, the concave wave is less obvious.

5.2 Influence of Detonation Mode on the Kinetic Energy Conversion Efficiency of the Shell

The formula for calculating the kinetic energy conversion rate of the shell is as follows [31]:

$$\eta = E1 / E2 \quad (6)$$

In the formula, η represents the conversion efficiency of shell kinetic energy, E1 represents the shell kinetic energy, and E2 represents the initial internal energy of the total explosive. In this paper, the initial internal energy of the total explosive includes the sum of the initial internal energy of the initiating explosive HMX, the inner explosive TNT and outer explosives CL-20 at 0 time. The kinetic energy value of the shell is selected from the maximum kinetic energy of the shell during the whole kinetic energy propagation process. The kinetic energy of the shell and the initial internal energy of the total explosive are originated from AUTODYN. In order to more clearly express the selection and location of the initial internal energy value of the total explosive and the kinetic energy value of the shell, the scheme 1 is taken as an example. As shown in Figure 10 and Figure 11, the selection and location of the initial internal energy value of the total explosive and the kinetic energy value of the shell in Scheme 1 are listed.

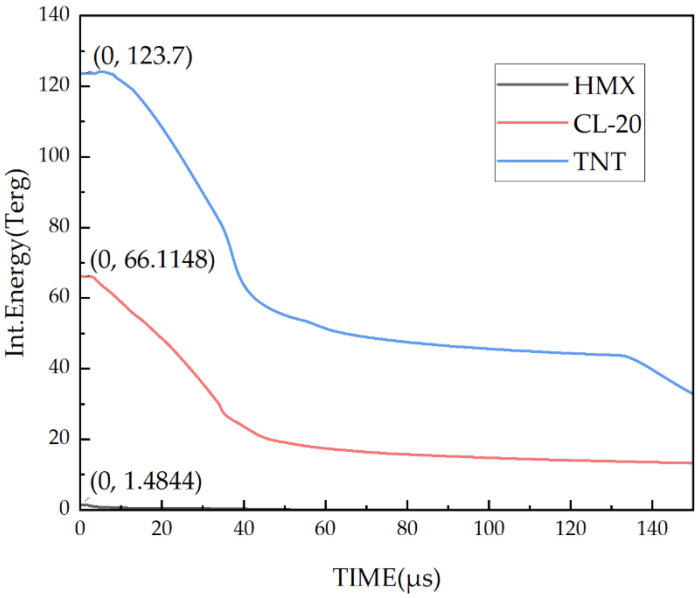

Figure 10. Initial Internal Energy Value of the Total Explosive in Scheme 1

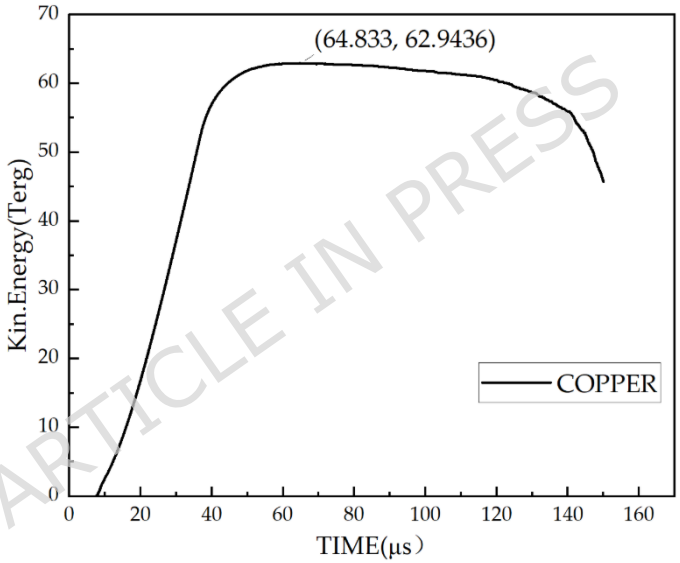

Figure 11. Kinetic Energy Value of Shell in Scheme 1

In the composite charge with the inner layer of all high detonation velocity explosives CL-20, the outer layer of all low detonation velocity explosives TNT, and the loading ratio of the inner and outer layers of explosives is 0.5, the effect of changing the initiation mode on the kinetic energy of the shell and the kinetic energy conversion efficiency of the shell is shown in Figures 12 and 13.

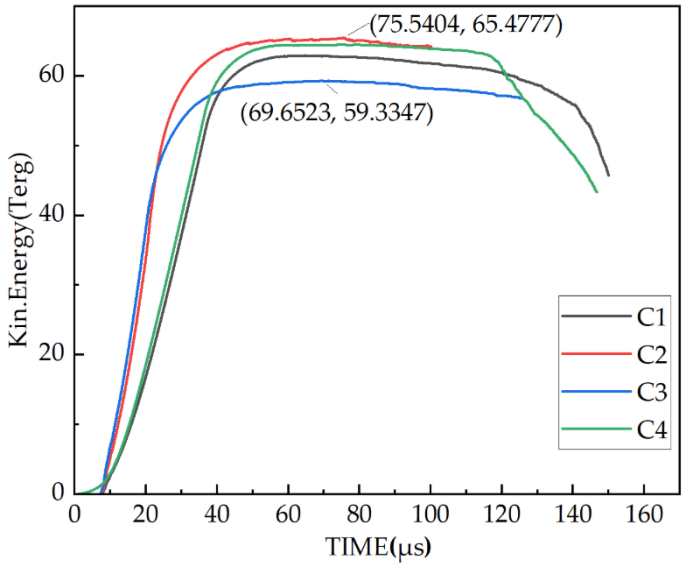

Figure 12. Influence of Detonation Mode on Kinetic Energy of Shell

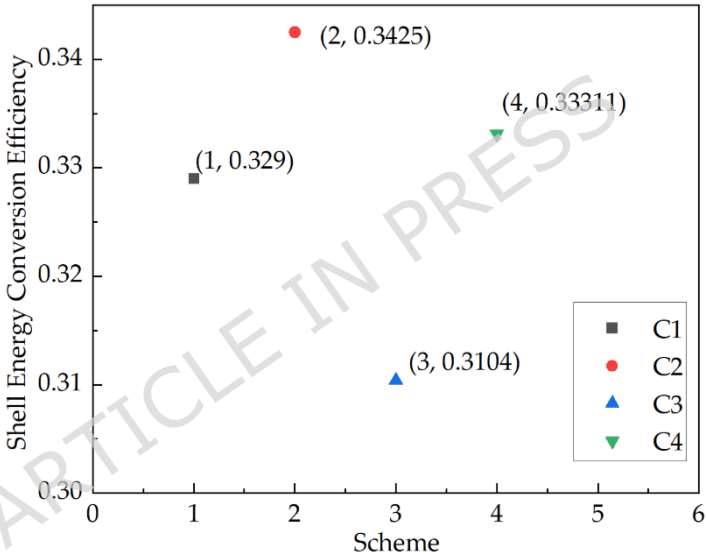

Figure 13. Influence of Detonation Mode on Kinetic Energy Conversion Efficiency of the Shell

It can be seen from Fig.12 that the kinetic energy of the shell propagates faster under the initiation of the center point at the bottom of both ends(C2), and the kinetic energy of the shell reaches the maximum value of 65.4777 Terg (1Terg = 1*1012J) among the four initiation modes. Under the internal center point initiation (C3), the propagation speed of kinetic energy is similar to the initiation of the center point at the bottom of both ends(C2), but the kinetic energy value of the shell is the smallest among the four initiation modes, only 59.3347 Terg. The maximum shell kinetic energy value is 10.35 % larger than the minimum kinetic energy value.

In the way of initiation of the center point at the bottom of one end (C1), the kinetic energy propagation speed is slow. Compared with the four initiation modes, the shell first obtains kinetic energy by initiation of the surface at the bottom of one end (C4), but the growth rate of kinetic energy is slow. It can be seen from Fig.13 that the kinetic energy conversion efficiency of the shell is up to 34.25 % under the initiation of the center point at the bottom of both ends(C2). The kinetic energy conversion efficiency of the shell obtained by the internal center point initiation(C3) is the lowest at 31.04 %, and the highest value is 10.34 % higher than the lowest value.

5.3Influence of the Charge Ratio on the kinetic energy conversion efficiency of the shell

In the composite charge with the inner layer of high detonation velocity explosive CL-20 and the outer layer of low detonation velocity explosive TNT, which is initiated by the center point at the bottom of one end, the influence of the charge ratio on the kinetic energy of the shell and the conversion efficiency of the kinetic energy of the shell is shown in Figure 14 and Figure 15.

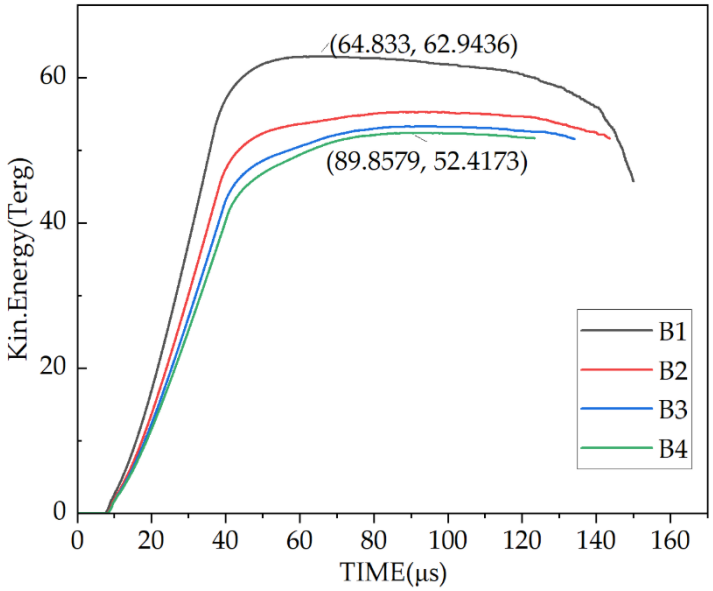

Figure 14. Influence of the Charge Ratio on the Kinetic Energy of the Shell

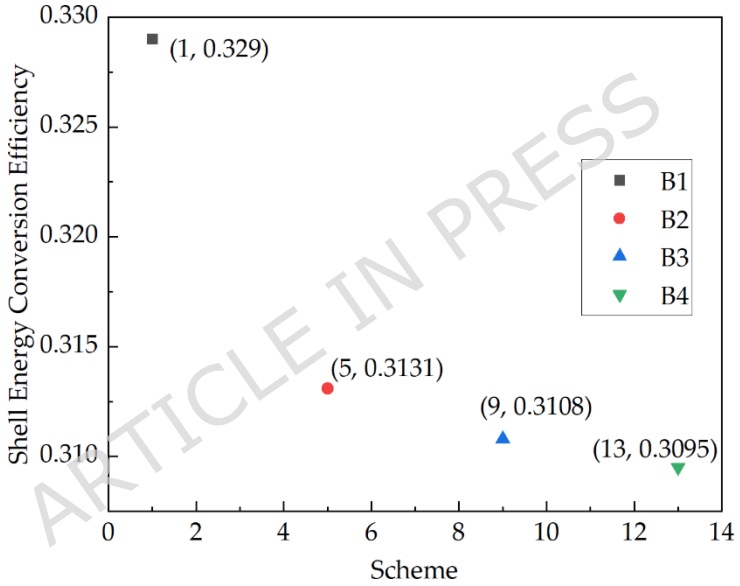

Figure 15. Influence of the Charge Ratio on the Conversion Efficiency of the Kinetic Energy of the Shell

As shown in Figure 14, when the loading ratio of inner and outer explosives is 0.5 (B1), the kinetic energy propagation speed is fast, and the shell kinetic energy value reaches the maximum value of 62.9436 Terg in the four charge ratios. When the loading ratio of inner and outer explosives is 0.2 (B4), the kinetic energy propagation speed of the shell is the slowest, and the kinetic energy value of the shell is the smallest of the four charge ratio schemes, which is 52.4173 Terg. The maximum shell kinetic energy value is 20.08 % larger than the minimum kinetic energy value. With the decrease of the loading ratio of the inner and outer explosives, the kinetic energy of the shell shows a significant downward trend. As shown in Figure 15, the kinetic energy conversion efficiency of the shell reaches a maximum value of 32.9 % under the condition that the loading ratio of the inner and outer explosives is 0.5. When the loading ratio of the inner and outer explosives is 0.2, the kinetic energy conversion efficiency of the shell reaches the lowest value of 30.95 %. The maximum shell kinetic energy conversion efficiency value is 6.3 % larger than the minimum value. With the decrease of the loading ratio of the inner and outer explosives, the kinetic energy conversion efficiency of the shell gradually decreases. In summary, for the composite charge with the matching relationship of inner high and outer low detonation velocity, and the loading ratio of inner and outer explosives is 0.5, the highest shell kinetic energy value and shell kinetic energy conversion efficiency can be obtained by initiating at the center point of both ends. Similarly, in the composite charge with high inner and low outer detonation velocity matching relationship and initiated by the center point at the bottom of one end, the highest shell kinetic energy value and shell kinetic energy conversion efficiency can be obtained when the loading ratio of inner and outer explosives is 0.5.

6 Multivariate Analysis Based on Orthogonal Optimization

In order to explore the influence of the initiation mode and the loading ratio of the inner and outer explosives on the kinetic energy conversion efficiency of the shell, the orthogonal optimization method is used for analysis.

6.1 Orthogonal optimization scheme design

The factor level design table is shown in Table 4. According to the size of the factors and the number of levels, the orthogonal table is selected to design the test scheme, and the parameter combination of the 16 tests is shown in Table 6.

Table 6. Test Scheme Design

Scheme Number	Detonation Velocity Maching Relationship A	Loading Ratio of Inner and Outer Explosives B (T1:T2)	Initiation Mode C
1	A1	B1	C1
2	A1	B2	C2
3	A1	B3	C3
4	A1	B4	C4
5	A2	B1	C2
6	A2	B2	C1
7	A2	B3	C4
8	A2	B4	C3
9	A1	B1	C3
0	A1	B2	C4
11	A1	B3	C1
12	A1	B4	C2
13	A2	B1	C4
14	A2	B2	C3
15	A2	B3	C2
16	A2	B4	C1

6.2 Analysis of Orthogonal Optimization Results

The 16 schemes of orthogonal test schemes listed in Table 6 are numerically simulated, and the results of shell kinetic energy conversion efficiency η and shell kinetic energy E1 are shown in Table 7.

Table 7. Numerical Simulation Results of 16 Schemes of Tests

Scheme Number	Factor			Test Index	
	1	2	3	η	E1(Terg)
	A	B	C		
1	A1	B1	C1	32.90%	62.944
2	A1	B2	C2	32.57%	57.478
3	A1	B3	C3	29.82%	51.185
4	A1	B4	C4	31.71%	54.645
5	A2	B1	C2	35.22%	86.455
6	A2	B2	C1	33.49%	86.959
7	A2	B3	C4	35.04%	92.381

8	A2	B4	C3	30.85%	82.365
9	A1	B1	C3	31.04%	59.335
10	A1	B2	C4	32.18%	57.8
11	A1	B3	C1	31.08%	53.33
12	A1	B4	C2	31.99%	54.254
13	A2	B1	C4	33.15%	81.083
14	A2	B2	C3	30.22%	78.601
15	A2	B3	C2	36.80%	97.493
16	A2	B4	C1	34.17%	91.174

In the 16 schemes of tests, the shell kinetic energy conversion efficiency and shell kinetic energy reached the maximum values in the 15th scheme of tests were: η = 36.8 % and E1 = 97.493, respectively, and the corresponding test combination was A2-B3-C2. The minimum shell kinetic energy conversion efficiency and shell kinetic energy occur in Scheme 3. Compared with the maximum shell kinetic energy conversion efficiency and the minimum shell kinetic energy conversion efficiency, the shell kinetic energy conversion efficiency increases by 23.41%. Compared with the maximum shell kinetic energy and the minimum shell kinetic energy, the shell kinetic energy increases by 90.47%.

Figures 16 and 17 are the average values of factors and levels obtained by range analysis of shell kinetic energy and shell kinetic energy conversion efficiency, respectively. Among them, in the part of detonation velocity matching relationship, the abscissa is 0.76 (Inner Low and Outer High) and 1.31 (Inner High and Outer Low) respectively. In the loading ratio of the inner and outer explosive, the abscissa is the loading ratio of the inner and outer explosive, which is 0.2,0.25,0.334 and 0.5, respectively. In the part of the initiation mode, the initiation mode cannot be expressed by specific numbers, so the four initiation modes are replaced by 1.0 (Initiation of the Center Point at the Bottom of One End), 2.0 (Initiation of the Center Point at the Bottom of Both End), 3.0 (Initiation of the Internal Center Point) and 4.0 (Initiation of the Surface at the Bottom of One End).

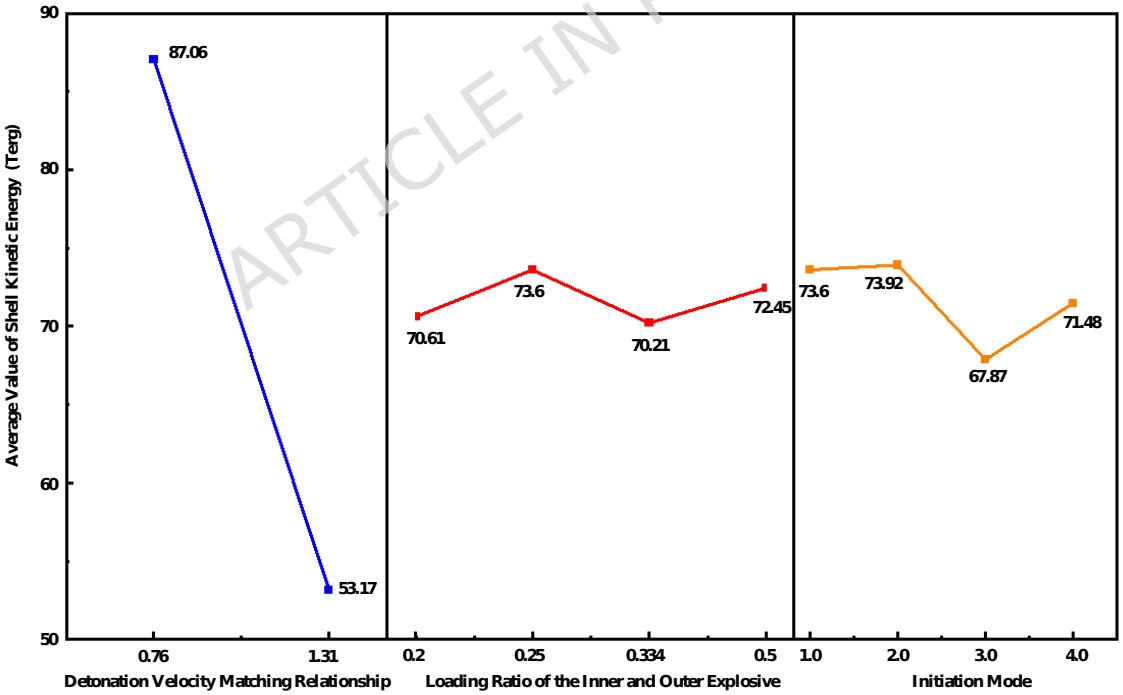

Figure 16. Figure of the Relationship Between the Average Value of Shell Kinetic Energy and the Level

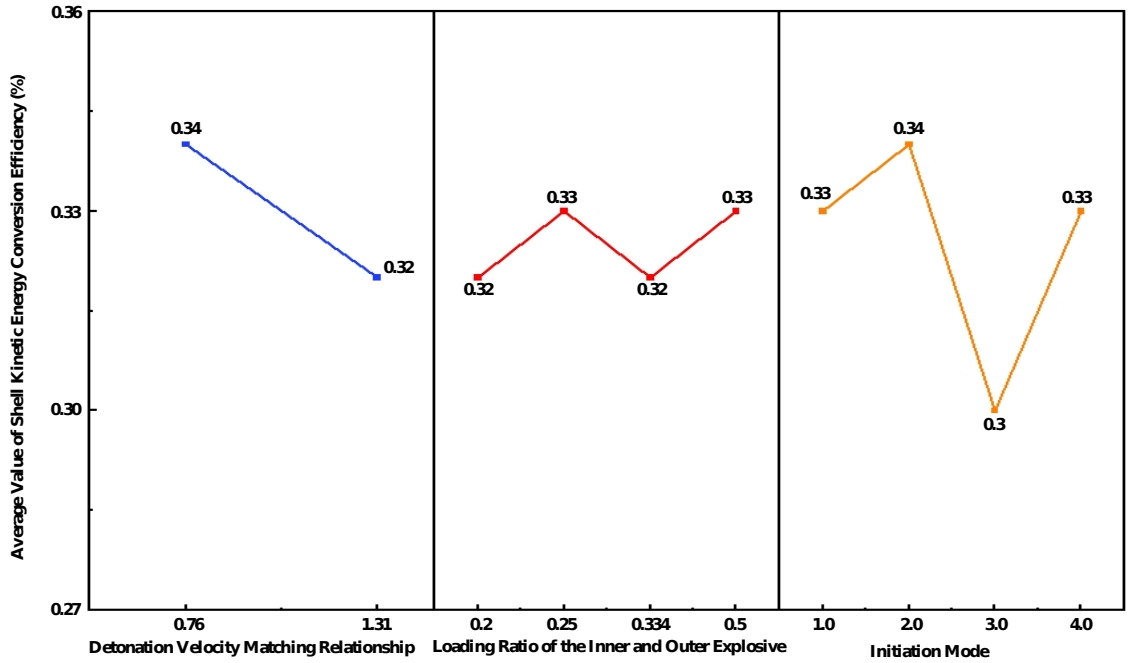

Figure 17. Figure of the Relationship Between the Average Value of Shell Kinetic Energy Conversion Efficiency and the Level

From Figure 16, it can be seen that when the detonation velocity matching relationship is the 0.76(Inner Low and Outer High), the loading ratio of the inner and outer explosives is the 0.25, and the initiation mode is the2.0(Initiation of the Center Point at the Bottom of Both Ends), the kinetic energy of the shell reaches the maximum value. It can be seen from Figure 17 that when the detonation velocity matching relationship is the 0.76 (Inner Low and Outer High), the loading ratio of the inner and outer explosives is the 0.25 or 0.5, and the initiation mode is the 2.0 (Initiation of the Center Point at the Bottom of Both Ends), the kinetic energy conversion efficiency of the shell reaches the maximum. By comprehensively analyzing the optimal level of the three factors in Figure 16 and Figure 17, the optimal level combination is determined to be A2-B3-C2.

7. Conclusions

In this paper, AUTODYN software is used to simulate and calculate the two kinds of detonation velocity matching relationship, four kinds of loading ratio of the inner and outer explosives, and the four kinds of initiation modes. Then, the detonation waveform diagram, shell kinetic energy and shell kinetic energy conversion efficiency are compared and analyzed. Orthogonal design was used to study the shell kinetic energy and shell kinetic energy conversion efficiency by three factors and levels of detonation velocity matching relationship, loading ratio of inner and outer explosives and initiation mode, so as to determine the best parameter combination scheme. Based on the research results, the following conclusions are drawn:

(1) Under the same matching relationship of inner high and outer low detonation velocity, the overall detonation waveform of composite charge is convex wave by changing the loading ratio of the inner and outer explosives and detonation mode. Under the matching relationship of inner low and outer high detonation velocity, changing the initiation mode and the loading ratio of inner and outer explosives, the overall detonation waveform is concave wave, and with the decrease of the loading ratio of inner and outer explosives, the concave wave is less obvious.

(2) In the composite charge with the matching relationship of inner high and outer low detonation velocity and the loading ratio of inner and outer explosives of 0.5, the kinetic energy propagation speed is fast under the initiation of the center point at the bottom of both ends, and the kinetic energy value of the shell and the kinetic energy conversion efficiency of the shell reach the maximum values of 65.4777 Terg and 34.25 %, respectively. In the way of internal center point initiation, the shell kinetic energy value and shell kinetic energy conversion efficiency are the smallest, which are 59.3347 Terg and 31.04 %, respectively.

(3) In the composite charge with the matching relationship of inner high and outer low detonation velocity and the initiation of the center point at the bottom of one end, when the loading ratio of the inner and outer explosives is 0.5, the kinetic energy propagation speed is fast, and the kinetic energy value of the shell and the kinetic energy conversion efficiency of the shell reach the maximum values of 62.9436 Terg and 32.9 %, respectively. When the loading ratio of inner and outer explosives is 0.2, the minimum shell kinetic energy value and shell kinetic energy conversion efficiency are 52.4173 Terg and

30.95 %, respectively. With the decrease of the loading ratio of the inner and outer explosives, the shell kinetic energy and the shell kinetic energy conversion efficiency gradually decrease.

(4) Through orthogonal optimization, the best combination of shell kinetic energy and shell kinetic energy conversion efficiency can be obtained as A2-B3-C2 (Inner Low and Outer High, Loading Ratio of the Inner and Outer Explosives is 0.25, and Initiation of the Center Point at the Bottom of Both Ends).

Author Contributions: Conceptualization, L.Z. and J.Y.; Methodology, L.Z.; Software, L.Z.; Validation, L.Z.; Investigation, L.Z. and X.L.; Experiment, L.Z.; Data curation, L.Z.; Writing—original draft preparation, L.Z.; Writing—review and editing, L.Z. and J.Y.; Supervision, L.Z.; Project administration, L.Z. All authors have read and agreed to the published version of the manuscript.

Funding: This research was funded by the Shanxi Province Basic research program free exploration category youth fund project, grant number 202203021212136; Supported by the China Postdoctoral Science Foundation under Grant Number 2024M760012; Supported by the Open Research Fund of Shanxi Key Laboratory of High-end Equipment Reliability Technology under Grant Number GDZBKKX—15.

Institutional Review Board Statement: Not applicable.

Informed Consent Statement: Not applicable.

Data Availability Statement: The data presented in this study are available on request from the corresponding author. The data are not publicly available due to programming privacy in structural design.

Conflicts of Interest: The authors declare that the research was conducted in the absence of any commercial or financial relationships that could be construed as a potential conflict of interest.

References

1. Gu, H.P.; Liu, W.; Li, G.J.; Influences of initiation modes on air blast wave fields produced by cylindrical explosives[J]. BLASTING, 2016,33(4): 34-38.
2. Li, D.W.; Kang, H.; Xiong, G.S.; Wang, X.F.; Wang, F.; Zhao, S.S.; Study on effects of initiation modes on pressure of shock wave[J]. Journal of Ordnance Equipment Engineering, 2021,42(5): 79-83.
3. Wang, L.;□Gao, X.J.; Li, X.H.; Gong, X.Z.;, The analysis of influence of detonation mode on warhead lithality[J]. Journal of Projectiles, Rockets, Missiles and Guidance, 2013,33(6): 86-88□203.
4. Miao, Y.S.; Guo, J.; Chen, X.; Wang, H.L.; Zhang, Y.P.; Sun, B.W.; Study on propagation characteristics of axial detonation wave of mining linear charges[J]. METAL MINE, 2022,(07):113-119.DOI:10.19614/j.cnki.jsks.202207015.
5. Deng, Y.X.; Zhang, X.F. Liu, C.; Li, P.C.; Ma, Z.W.; Liu, Z.H.; Effect of initiation models on the fragment velocity distribution of elliptical cross-section warhead[J]. EXPLOSION AND SHOCK WAVES, 2024,44(10):98-112.
6. Guo, J.; SUN, B.W; Yao Y.K; Wang, H.L; Miu Y.S; Zhang, Y.P; Study of the effect of initiation method on the propagation characteristics of detonation wave[J]. Journal of Qingdao University of Technology, 2024,45(03):35-42.
7. Xiao, X.; Zhang, J.H.; Wu, F.; Lei, X.L.; Numerical Simulation and Experimental Study of Double Groove Shaped Charge Detonated by Two Initiations[J]. BLASTING , 2015,32(01):38-42.
8. Li, Y.J.; Miu, Y.S; Li, B.; Huang, F.F.; Ge, S.; Yang, T.; Wu, J.Y.; Characteristics of Axial Propagation of Detonation Waves in Symmetric Bilinear Detonation[J]. Explosive Materials, 2025,54(1): 7-13.
9. Jun-bao Li, Wei-bing Li,Xiao-ming Wang,et al. Influence of combination of coaxial cylindrical explosives on fragmentation and shock waves of a shelled composite charge[J]. Propellants, Explosives, Pyrotechnics,2023,Vol.48(6): e202200318.
10. Zhang, G.H.; Shen, F.; Liu, R.; Wang, H.; Influence of Detonation Modes on Energy Release Characteristics of a Charge with a Non-Circular Cross-Sectional Structure[J]. Chinese Journal of High Pressure Physics, 2022,36(3): 129-137.
11. Deng, H.; Quan, J.L.; Liang, Z, F.; Influence of eccentric initiation on energy distribution gain of a warhead charge[J].
Explosion and Shock Waves, 2022,42(05):3-15.
12. Zhang, S.F.; Numerical simulation study on detonation energy output and shock wave sensitivity of composite char[D]. Nanjing University of Science and Technology,2010.
13. Yin, J.T.; Wei, H.J.; Li, B.H.; Fu, W.; Explosion characteristics of Metal Accelerating Explosive/ High Detonation Heat Explosive Composite Charge[J]. Initiators & Pyrotechnics, 2015(03):33-37.
14. Niu, Y.L.; Wang, X.F.; Yu, R.; Characteristic of Energy Output of Under Water Explosion for Dual Explosive Charge[J]. CHINESE JOURNAL OF ENERGETIC MATERIALS, 2009,17(04):415-419.
15. Shen, F.; Wang, H.; Wang, J.T.; Yu, W.L.; Wang, X.J.; Detonation driving energy release characteristics of laminated composite charge of DNTF-based aluminized explosives based on cylinder tests[J]. Explosion and Shock Waves, 2023,43(11):56-64.

16. T.Hamada,Y.Nakamura,K.Murata. The Performance of Pressure Vessel Using Concentric Double Cylindrical High Explosive[C]. ASME Pressure Vessels & Piping Conference, Cleveland, USA, July 20-24,2003:319-326.
17. Shi, L.P.; Wang, C.L.; Wu, H.B.; Shi, W.Q.; Xue, Z.Q.; Enhancement Effect of Initiation Methods on Shock Wave Power in Near-Ground Field Explosive[J]. Transactions of Beijing Institute of Technology,2022,42(4): 340-346.
18. Li, J.B.; Li, W.B.; Wang, X.M.; Li, W.B.; Characteristic of fragment for shelled coaxial ternary composite charge[J]. Journal of Nanjing University of Science and Technology, 2022,46(5): 515-522.
19. Shen, F.; Luo, Y.M.; Yu, W.L.; Wang, X.J.; Experimental Study on Propagation Characteristics of Detonation Wave of Typical Coaxial Binary Charges[J]. Chinese Journal of Explosives & Propellants. 2022,45(03):412-418.DOI:10.14077/j.issn.1007-7812.202202002.
20. Wang, Z.Y.; Study on initiation of PBX explosive under impact load[D]. North University of China, 2023.DOI:10.27470/d.cnki.ghbgc.2023.000136.
21. Ling, Q.; He, Y.; He, Y.; Zhou, J.; Numerical Simulation of Directed Scattering of Fragments Driven by Sector-Shaped Double-Layer Charge[J]. Chinese Journal of High Pressure Physics, 2017,31(05):557-565.
22. Lu, F.Y.; Li, X.C.; Wen, X.J.; Chen, R.; Cao, L.; Theoretical Analysis on Flying Velocity of Double Layer Fragments Driven by Small Charge Ratio Explosion[J]. Modern Applied Physics, 2018,9(4):25-31.
23. Zhao, Z.J.; Li, W.B.; Li, J.B.; Li, W.B.; Wang, X.M.; Effects of Composite Shaped Charge with Wave Shaper on Formation of Double-layer Liner Penetrator. Chinese Journal of Explosives & Propellants, 2024,47(04):344-353.DOI:10.14077/j.issn.1007-7812.202307004.
24. Shen, Y.M.; Fragmentation Characteristics of Composite Charge Warhead and Its Influencing Factors Research[D]. Nanjing University of Science and Technology, 2024.DOI:10.27241/d.cnki.gnjgu.2021.003335.
25. Li□D. D; Numerical Simulation of Critical Combustion and Explosion Characteristics of Typical Double-base Propellants[D]. NANJING UNIVERSITY OF SCIENCE & TECHNOLOGY, 2023.DOI:10.27241/d.cnki.gnjgu.2023.001105.
26. Zhang, C.P.; Zhang, X.F.; Tan, M.T.; Hou, X.W.; Xiong, W.; Liu, C.; Gu, X.H.; Experimental and Numerical Simulation of Shaped Charge Jet Penetrating Concrete and Rock Targets[J]. Chinese Journal of Energetic Materials, 2023,31(8):773-785.
27. Shen, Y.M; Li W.B.; Cao,Y.J.; Li, J.B.; Wang, X.M.; Influence of Structural Parameters on Characteristics of Fragments from Warheads with a Composite Charge[J].Chinese Journal of Energetic Materials□Hanneng Cailiao□,2022,30(1):50-57.
28. Chen, C.L.; Ma, K.; Yang, J.C.; Cao, J.; Yin, L.X.; Feng, N.; Gao, P.F.; Wang, C.X.;, Li, S.; Zhou, G.; Qian, B.W.; Johnson-Cook Constitutive Model and Failure Parameters of Al-Based Energetic Structural Material[J]. Chinese Journal of Solid Mechanics, 2023,44(6):782-794.
29. Jiaxin Yu, Weibing LiCA1, Junbao Li, et al. The detonation wave propagation and the calculation methods for shock wave overpressure distribution of composite charges[J]. Defence Technology, 2025,Vol.48: 204-220.
30. Wang, M.T.; Cheng, Y.H.; Wu, H.; Study on blast loadings of cylindrical charges air explosion[J]. Explosion and Shock Wave, 2024,44(04):62-82.
31. Yang, Y.S.; Wang, W.; Wang, X,; Chen, Z.Y.; Liu, J.Z.; Theoretical Calculation of Energy Conversion Efficiency ofβ-Photovoltaic Battery. Instrumentation, 2021,28(1): 76-80.
32. Zhang, J.; Li, Y.C.; Huang, J.Y.; Wu, J.X.; Sun, H.; Ren, X.X.; Orthogonal Optimization Design of Shaped Charge Structure for Underwater Blasting[J]. Journal of Ordnance Equipment Engineering, 2021,42(2): 52-57.
33. Sui, S.Y.; Wang, S.S.; Terminal Effects[M]. Bei Jing□National Defense Industry Press□1999: 280.
34. Yuan, J.M.; Xia, T.; Yu, Y.W.; Zhao, W.; Qu, Y.; Cao, X.; Virtual Simulation Experiment of Detonation Velocity Test for Explosive Basedon Numerical Simulation[J]. Research and Exploration In Laboratory, 2022,41(03):111-115+160.DOI:10.19927/j.cnki.syyt.2022.03.022.
35. Hu, Y.F.; Zhang, H.L.; Chen, Z.Q.; Li, W.B.; Ning, X.L. Numerical Simulation Research on Warhead Fragmentation Shape and Fragments Scattering Characteristics[J]. Journal of Ordnance Equipment Engineering, 2024,45(05), 72-78.